Numerical Investigation of Turbulent Hydrogen-Methane-Nitrogen Non-Premixed Jet Flame

B. Sungur, B. Topaloglu[*(Corresponding author)], H. Ozcan, L. Namli

Mechanical Engineering Department, Ondokuz Mayis University, Samsun, Turkey

Abstract

In this work, the numerical investigation of the two-dimensional axisymmetric turbulent diffusion flame of a composite fuel was performed by using a computational fluid dynamics code to predict flame structure. The composite fuel was an $H_2/CH_4/N_2$ gas mixture. The amount of H_2 and N_2 in the fuel mixture varies under constant volumetric fuel flow rate. Fluent, which solves the governing and reaction equations using the finite volume method, was used as the computational fluid dynamics program. The non-premixed model was used for computation of the combustion. The standard k-ε model was used for modeling the turbulent flow. The interaction of the chemistry and turbulence was accounted for by the program with the probability density function model. This model was validated against the experimental data taken from literature. In general, the numerical results of the temperature, velocity, and CO_2 concentration distributions were in satisfactory agreement with the experimental results. The numerical results showed that adding H_2 to the fuel mixture decreases the flame length and generally increases the maximum temperature of the flame. On the other hand, adding N_2 to the mixture decreases both the flame length and maximum flame temperature. The flame length corresponds to the axial position of the peak flame temperature.

Keywords: Combustion Modeling; Composite Fuels; Diffusion Flame; $H_2/CH_4/N_2$ Flame; Flame Length; Emissions

1. Introduction

Emissions of the fossil fuels like carbondioxyde (CO_2), carbonmonoxyde (CO), nitrousoxides (NO_x) etc. are harmful to the environment and increase the global warming. These problems of the fossil fuels have prompted to countries to use alternative energy sources and to use the available energy sources more efficiently, as well. At this point composite fuels have increased their importance recently. Composite fuels provide many useful features on flame, emissions and economy. Especially the choice of hydrocarbon-hydrogen flames is an attractive way for reducing dependency on fossil fuels. In recent years, there have been attempts at enriching various gaseous fuels such as natural gas or propane with H_2. Adding hydrogen to a fuel stabilizes the flame, improves ignitability and flame holding, and reduces pollutant emissions, with the exception of NO_x. These positive effects are undoubtedly valid for alternative fuels such as biogas, landfill gas, or syngas with high content of CO_2 or N_2, which reduces the heating values and worsens the flammability.

For the investigation of complex physical and chemical processes in non-premixed flames of composite fuels, experimental studies are essential. In recent times, very powerful measurement methods have been developed and applied. In particular, non-intrusive optical methods such as Rayleigh or Raman scattering, laser-induced fluorescence (LIF), or particle imaging velocimetry allow measurement results with high temporal and spatial resolution (Bergmann et al., 1998). However, such measurements are generally very expensive and require much time.

Computational fluid dynamic (CFD) programs can simulate the combustion processes rapidly and economically. During combustion, the mass, momentum, and energy transfers occur together. Continuity, momentum, energy, and species conservation equations are non-linear partial differential equations and their analytical solutions are very difficult or impossible except under simple conditions. These equations were solved with the computational methods (Fluent, 2006). CFD programs are widely used in studies of combustion reactions to model the flame, flow, and pollutant emissions. Neuber et al. (1998) carried out a numerical and experimental study in order to investigate the turbulent diffusion combustion of pure hydrogen fuel. They modelled turbulent flow in a combuster with using standard k-ε model, and also used the probability density function (PDF) method to solve the turbulence−chemistry interaction. They reported that the model gave good flow predictions. Zhou et al. (2000) modeled a hydrogen/air diffusion flame using the standard k-ε model with Rodi's correction, a detailed chemical mechanism obtained from the CHEMKIN-II package and an algebraic correlation closure model for the coupling of turbulence and chemistry. They observed that temperature and H_2, O_2, H_2O, and N_2 concentrations were in good agreement with the experimental data taken from literature. Francis et al. (2011)

performed numerical and experimental investigations of the structure and the reaction zones of unconfined methane−hydrogen laminar jet diffusion flames. They found that hydrogen increased fuel burning rate and thereby decreased overall visible flame extent. Ilbas et al. (2005) numerically investigated the turbulent non-premixed hydrogen and hydrogen−hydrocarbon flames in a small burner. They observed that temperature and main pollutant concentrations (CO ve NO_x) were in good agreement with the experimental results. Frassoldati et al. (2005) used the commercial code Fluent to investigate a high swirl, confined natural gas diffusion flame by referring to the work developed within the German TECFLAM. They observed that the CFD simulation showed satisfactory agreement with the measured data. Khelil et al. (2009) performed numerical simulations of a high swirl, non-premixed, confined natural gas diffusion flame to predict NO_x emissions, and they used a PDF model with a Reynolds stress model (RSM). According to their findings, the peak of the temperature in the inner recirculation zone of the flame was underestimated.

El-Ghafour et al. (2010) investigated experimentally the combustion characteristics and flame structure of natural gas−hydrogen composite fuel in a free jet turbulent diffusion flame. They observed that adding hydrogen to natural gas leads to higher combustion temperatures. Choudhuri et al. (2003) studied the characteristics of hydrogen−natural gas composite fuel in turbulent jet flames located in a vertical combustion chamber. They demonstrated that adding hydrogen to the fuel mixture decreased the visible flame length, the radiative heat release factor, and the emissions of CO and soot, but increased the emission of NO_x. Tabet et al. (2009) analyzed the structure of turbulent non-premixed CH_4-H_2/air flames with a special emphasis on mixing and air entrainment. Their analysis showed that hydrogen addition improved the mixing, air entrainment, and CH_4 consumption and so reduced the flame length and thickness as a consequence of the intensification of the combustion process.

In most of the aforementioned studies, investigators focused on the combustion of hydrogen−hydrocarbon fuel mixtures. However, it is apparent that the literature contains little information on the flame structure of fuel mixtures containing H_2/CH_4 and N_2. Therefore, the flame structure of a H_2/CH_4/N_2 fuel mixture was studied in this work. The present study consists of two parts. In the first part, the temperature, axial velocity, and CO_2 concentrations of the turbulent diffusion flame of an H_2/CH_4/N_2 composite fuel with a specific content of 33.2% H_2, 22.1% CH_4, and 44.7% N_2 (by volume) were numerically calculated and the results compared with the data taken from literature (Sandia, 2013) for validation. In the second part, the effect of varying the hydrogen and nitrogen content in the mixture on combustion was investigated numerically. The commercial code Fluent was used to simulate the problem.

2. Modeling of Turbulent Non-Premixed Combustion

Fluent code uses the finite volume method to convert the partial differential equations (continuity, momentum, energy, and species) into algebraic equations and solve these equations. The general form of the steady-state transport equation for the 2D turbulent reactive flow under cylindrical coordinates can be written as:

$$\frac{\partial}{\partial x}(\rho u \phi) + \frac{1}{r}\frac{\partial}{\partial r}(r\rho v \phi) = \frac{\partial}{\partial x}\left(\Gamma \frac{\partial \phi}{\partial x}\right) + \frac{1}{r}\frac{\partial}{\partial r}\left(r\Gamma \frac{\partial \phi}{\partial r}\right) + S_\phi \tag{1}$$

where ϕ denotes 1, u, v, k, ε, h, Y_i and the general diffusion coefficient Γ is in turn 0, μ_t, μ_t, $\frac{\mu_{eff}}{\sigma_k}$,

$\frac{\mu_{eff}}{\sigma_\varepsilon}$, $\frac{\lambda}{c_p} + \frac{\mu_t}{\sigma_h}$ and $\rho D_{im} + \frac{\mu_t}{\sigma_Y}$, respectively.

A fuel and an oxidizer enter the reaction zone in distinct streams in non-premixed combustion. The non-premixed modeling approach contains the solution of transport equations for one or two conserved scalars (the mixture fractions). It is not necessary to solve equations for individual species because species concentrations are derived from the predicted mixture fraction fields. Interaction of the turbulence and chemistry is calculated with a PDF. The non-premixed combustion modeling approximation was improved especially for the simulation of turbulent diffusion flames with fast chemistry. This model also permits intermediate species prediction, dissociation effects, and rigorous turbulence−chemistry coupling. It is possible to model the chemistry as being in chemical equilibrium with the equilibrium model, being near chemical equilibrium with the steady laminar flamelet model, or significantly departing from chemical equilibrium with the unsteady laminar flamelet model.

It is assumed that the chemistry is rapid enough for chemical equilibrium to exist always at the molecular level in the equilibrium model. An algorithm that is based on the minimization of Gibbs free energy is used to account for species mole fractions from the mixture fraction (Fluent, 2006).

3. Numerical Solution and Model Validation

3.1. Validation of the Numerical Results

The experiments of a turbulent diffusion flame of an $H_2/CH_4/N_2$ composite fuel flame, which have been used for model validation, were carried out by Meier et al. (2000). In that experimental study, Raman signals and laser-induced fluorescence (LIF) were used for determining the concentrations of the major species and minor species (OH, NO, CO), respectively. On the other hand, Rayleigh signals were used to measure the temperatures. The burner consisted of a straight stainless steel tube with a length of 35 cm and an inner diameter of 8 mm (Figure 1). The outside of the tube was surrounded by a nozzle with an inner diameter of 140 mm. This nozzle was used for supplying the co-flowing dry air to the lower part of the flame at an exit velocity of typically 0.3 m/s. Fuel exited from the inner tube with the exit velocity of 42.2 m/s. The fuel was a mixture of 33.2% H_2, 22.1% CH_4, and 44.7% N_2 (by volume). The Reynolds number of the fuel jet in the inlet section was 15200. Measurements were performed at six heights above the nozzle at $x/D=$ 5; 10; 20; 40; 60, and 80. The details of the experiments such as procedures, equipments and fundamentals of the measuring techniques have been given in (Bergmann et al., 1998).

3.2. Numerical Solution Parameters and Boundary Conditions

In this work, simulations were performed using a pressure-based, steady state, segregated implicit solver. The relationship between velocity and pressure corrections was calculated with the SIMPLE algorithm (Patankar, 1980). As the combustion model, the non-premixed model was used with an equilibrium assumption. For the turbulence modeling, the standard k-ε model was selected. For modeling of the radiation effect, the P1 approach was used. But there was no significant difference between the model using this approach and the one in which this approach was not used. Therefore, the calculations were performed without radiation.

Figure 1. A photograph of the burner with the flame (Sandia, 2013)

For the numerical solution, the geometry must be enclosed with the grid. The grid's length is in axial distance 1200 mm and in radial distance 200 mm (Figure 2). Due to axial symmetry, only half of the flame plane was

simulated. As shown in Figure 2, critical zones were meshed with a fine grid, where fuel and air mixing zones were close to the burner and all physical and chemical gradients changed rapidly. This non-uniform grid had 57,200 meshes. To see the grid more clearly, the first half of the grid in the axial direction was shown. The other half continues as the end zone of the first half. Also, more grid structures were tested to see the grid's effect on the solution. Very fine grids having constant edge lengths of 0.8 mm and 0.4 mm with 375,000 and 1,500,000 meshes, respectively, were also used for calculations. However, in these calculations with more grids, there were no meaningful changes in the results; consequently, all calculations were performed with the grid with 57,200 meshes.
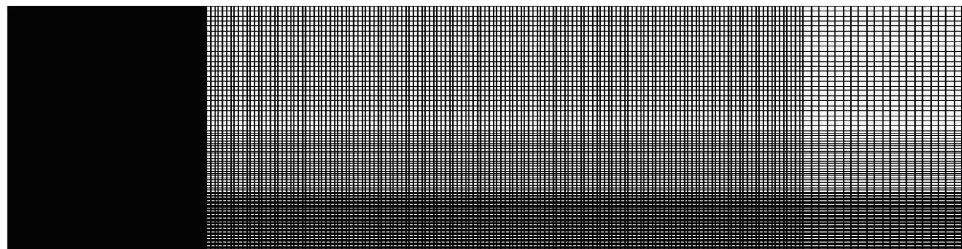
Figure 2. Grid used in this study

Fuel inlet velocity and temperature were 42.2 m/s and 292 K and air inlet velocity and temperature were 0.3 m/s and 292 K, respectively. Fuel composition was defined by 33.2 % H_2, 22.1 % CH_4, and 44.7 % N_2 as volumetric proportion. The burner was symmetric, so axial symmetry conditions were defined at the axis. Exit zone was defined by the pressure outlet. At the outer boundary of the combustion zone, all the conditions were defined as symmetry.

Continuity, momentum, energy, and species governing equations were solved iteratively until the convergence was obtained. Convergence was considered to be reached after the residuals of all governing and transport equations were less than 10^{-6}.

After model validation, the flame structure calculations were performed by varying the fuel composition for the same geometry and boundary conditions in the calculations with constant volumetric fuel flow rate. During the calculations with the same energy rate, the fuel inlet velocity was adjusted adequately.

4. Results and Discussion

4.1. Comparison of the Experimental and the Numerical Results

The measured and predicted temperature contour graphs are presented in Figure 3. As shown in this figure, the maximum temperature values in the numerical simulation were in the range of x/d ≈ 41−60, r/d ≈ 0−2. In the experimental study, maximum temperature values were in the range of x/d ≈ 52−63, r/d ≈ 0−1.2. In regions close to the burner, temperature values were low because the flame just began to occur. Flame temperature values increased in the region where the air−fuel ratio came near to the stoichiometric mixture ratio. In the experimental study, effective flame length and flame width were lower than they were in the numerical simulation. The experimental and the numerical results were in satisfactory agreement, as shown in Figure 3.
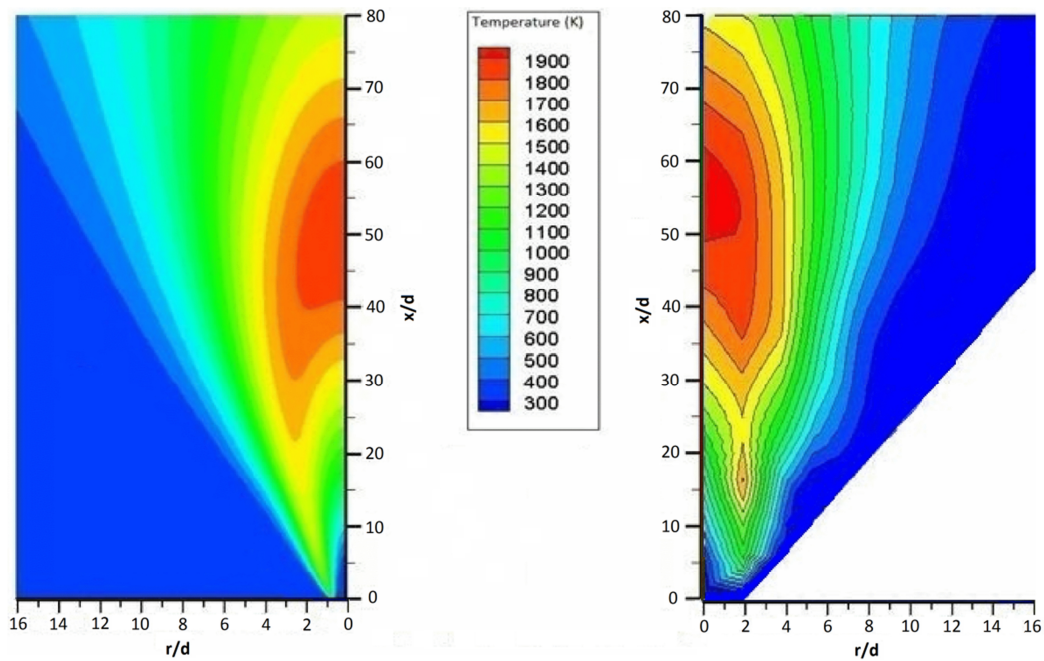
Figure 3. Predicted (left) and measured (Sandia, 2013) (right) temperature distribution

To make a more detailed comparison, the measured and predicted radial temperature profiles in different axial distances were presented in Figure 4. In the numerical simulation at the value of x/d = 5, the highest temperature value was at r/d ≈ 1.2; after this value, with the increasing r/d, temperature values decreased. In the experiments, the highest temperature value was at r/d ≈ 1.2, and after this value, with increasing r/d, temperature values decreased. Between r/d = 0 and r/d ≈ 0.8, the measured and predicted temperature values were in good agreement. In the numerical simulation at the value of x/d = 20, the highest temperature value was at r/d ≈ 2.3, and after this value, with increasing r/d, temperature values decreased. In the experiments, the highest temperature value was at r/d ≈ 1.5, and after this value, with increasing r/d, temperature values decreased. Between r/d ≈ 1 and r/d ≈ 2.2, the measured and predicted temperature values were in good agreement. At the value of x/d = 40, the highest temperature values for numerical and experimental results were at r/d ≈ 2.2, and after this value, with increasing r/d, temperature values decreased. Between r/d ≈ 0 and r/d ≈ 2.5, the measured and predicted temperature values are in good agreement. At the value of x/d = 80, the highest temperature values for numerical and experimental results were at r/d = 0, and after these values, with increasing r/d, temperature values decreased.
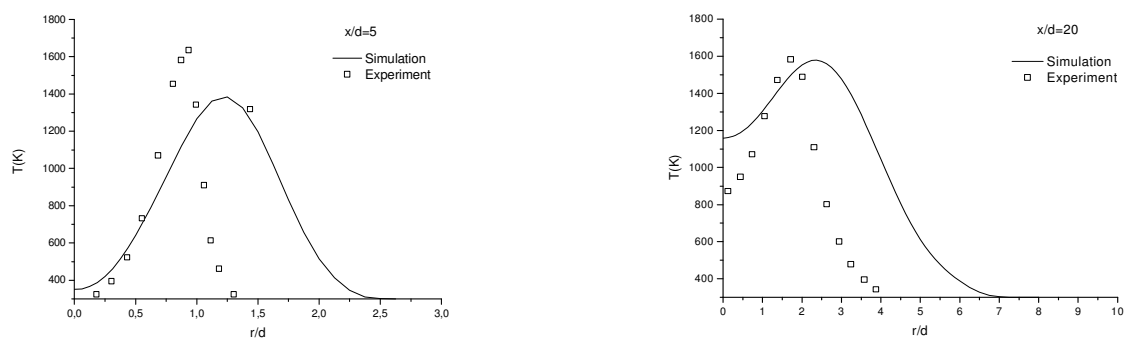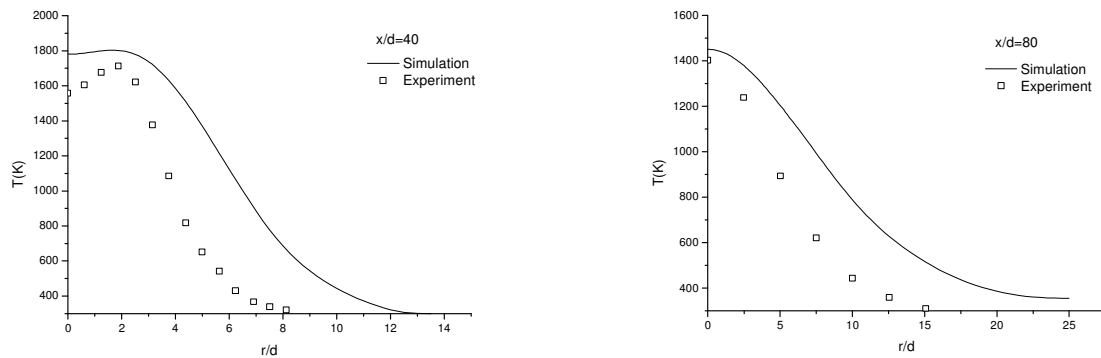
Figure 4. Predicted and measured (Sandia, 2013) temperature profiles (x/d = 5, x/d = 20, x/d = 40, x/d = 80)

In general, the predicted temperature values were higher than the experimental results. This deviation is due to the fact that combustion is a difficult and complex process to model and the reaction mechanism cannot exactly reflect the real combustion. Besides, this deviation occurs because of the equilibrium assumption in the non-premixed and turbulence models that are used in the simulation.

The measured and predicted axial velocity contour graphs are presented in Figure 5. As shown in this figure, the experimental and numerical results were in satisfactory agreement as a distribution. But in the experimental results, the axial velocity values were higher than the numerical results. Also, it was obtained that axial velocity values decreased with increasing r/d.
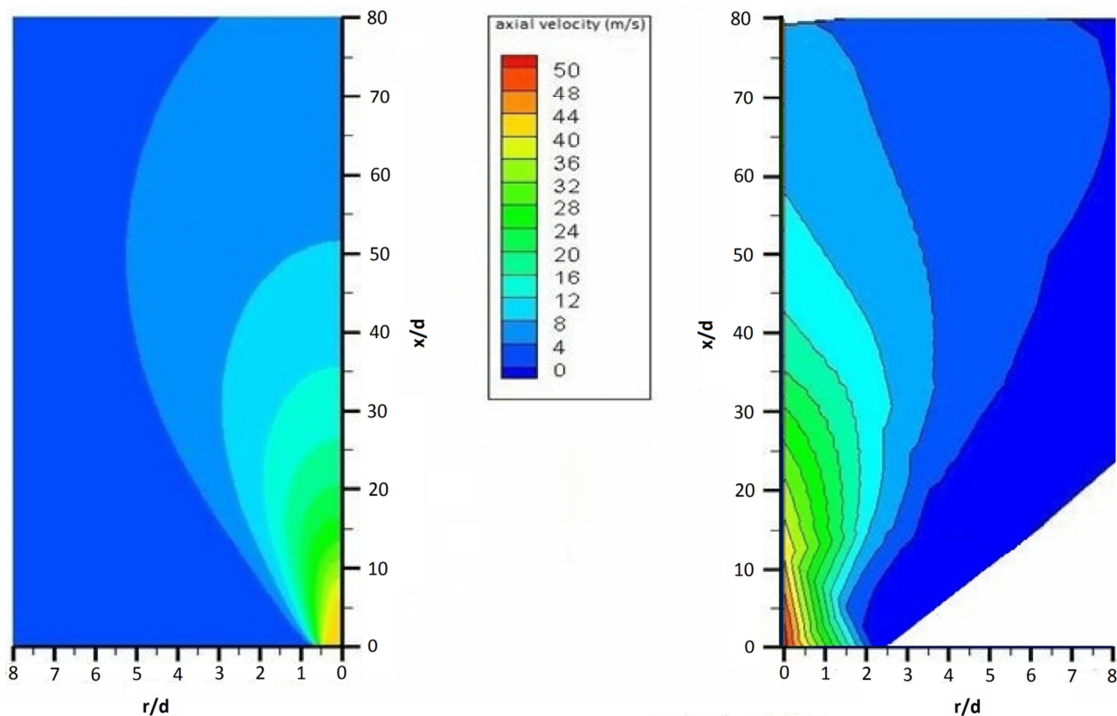
Figure 5. Predicted (left) and measured (Sandia, 2013) (right) axial velocity distribution

Again, to make a more detailed comparison, the measured and predicted axial velocity profiles at radial coordinates in different axial distances are presented in Figure 6. As shown in this figure, with increasing r/d, the measured and predicted axial velocity values decreased. Also at the values of x/d = 5, x/d = 20 and x/d = 40, the

numerical results were higher than the experimental results until r/d's certain value; after this value, the numerical results were higher than the experimental results. At the value of x/d = 80, the experimental results were higher than the numerical results for all r/d values.

In the following, the CO_2 concentration distribution is presented only with contour graphs. Their profiles were not given to save space in the paper. The measured and predicted CO_2 concentration contour graphs are presented in Figure 7.

As shown Figure 7, in the numerical simulation the maximum CO_2 values were at the range of x/d ≈ 53−59, r/d ≈ 0−1. In the experimental study, the maximum CO_2 values were at the range of x/d ≈ 59−65, r/d ≈ 0−0.7. Generally, in collaboration of temperature distribution, predicted CO_2 concentration values were higher than the experimental results. Also, in regions close to the burner, CO_2 concentration values were low, because the flame just began to occur and hence products had not yet occurred.

4.2. Flame Structure Results

The flame structure calculations were performed numerically in the case of 0%N_2 with varying hydrogen content from 0% to 100%, 15%N_2 with varying hydrogen content from 0% to 85%, 30%N_2 with varying hydrogen content from 0% to 70%, and 45%N_2 with varying hydrogen content from 0% to 55% conditions at constant volumetric flow rate. Also, calculations were performed at 15%N_2, 30%N_2, and 45% N_2 with varying volumetric flow rate of fuel to give the same energy as those provided under 0% N_2 conditions.

Figure 8 shows temperature contour graphs of varying methane−hydrogen flame in the case of %45 N_2 conditions.
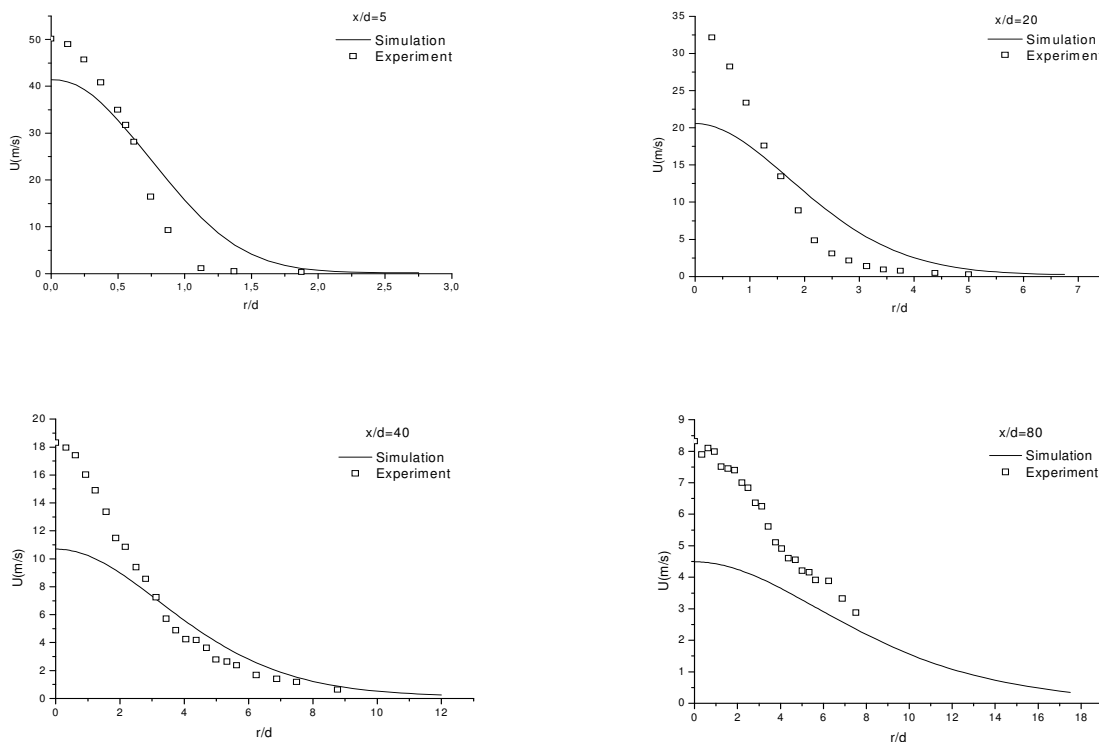
Figure 6. Predicted and measured (Sandia, 2013) axial velocity profiles (x/d = 5, x/d = 20, x/d = 40, x/d = 80)
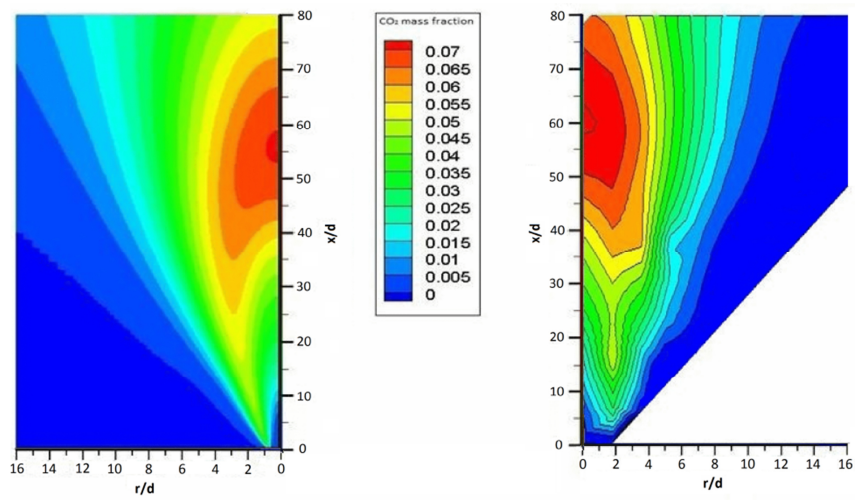
Figure 7. Predicted (left) and measured (Sandia, 2013) (right) CO_2 concentration distribution
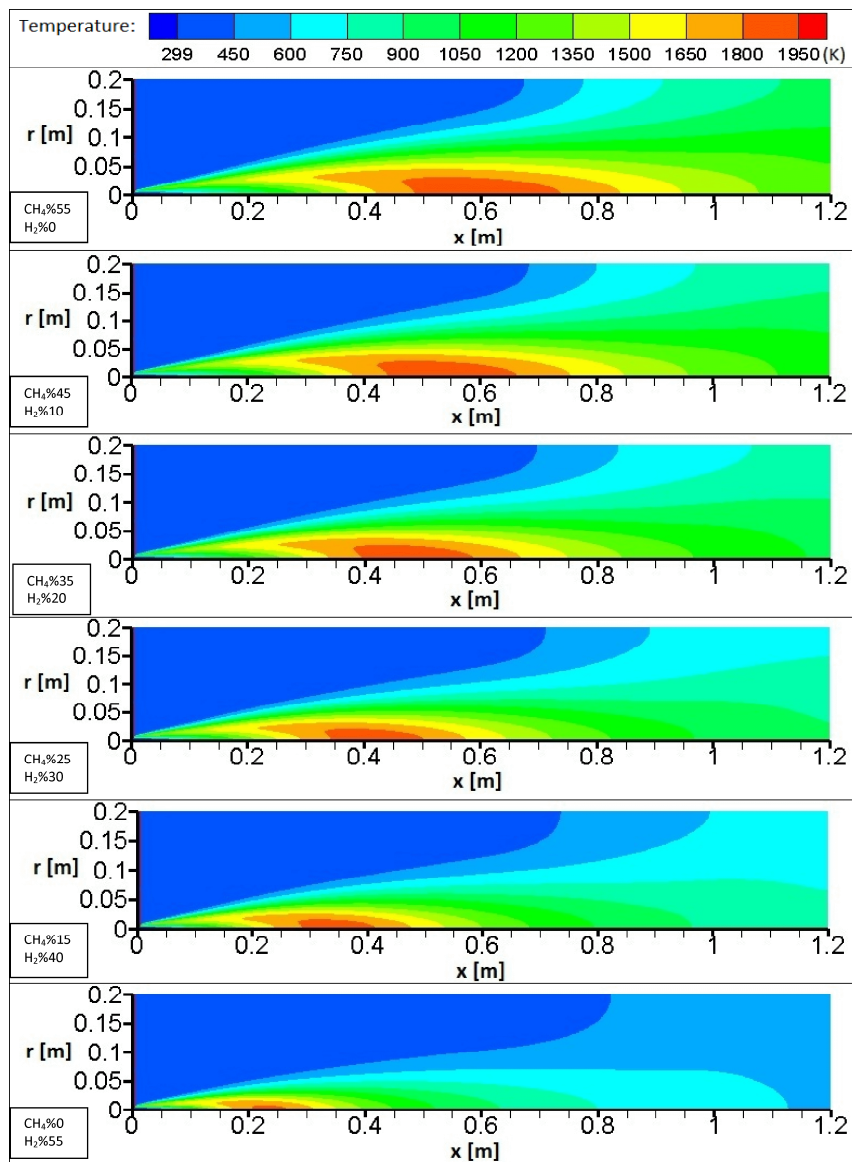
Figure 8. Predicted temperature distribution at %45 N_2 conditions

From this figure, it can be observed that adding hydrogen to the mixture reduces the flame length. For other cases with 0%N_2 to 30%N_2 content, results similar to those in Figure 8 were obtained. In Figure 9, centerline temperature profiles in the axial direction for all cases are shown. From this figure, it can be observed that adding nitrogen besides hydrogen also reduces the flame length. The reason for this behavior is the reduced stoichiometric air fuel ratio, so that the fuel travels a shorter distance with air before combusting. Furthermore, with the increase of hydrogen content in the mixture, the chain-carrying radicals such as H, O, and OH increase and enhance the combustion rate. As a total effect, the composite fuels with hydrogen content burn faster and reduce the flame length. Adding hydrogen generally increases the maximum flame temperature. This increase continuously decreases with increasing nitrogen content, so that last, in the case of %45 N_2 conditions, the maximum flame temperature decreases despite hydrogen addition.
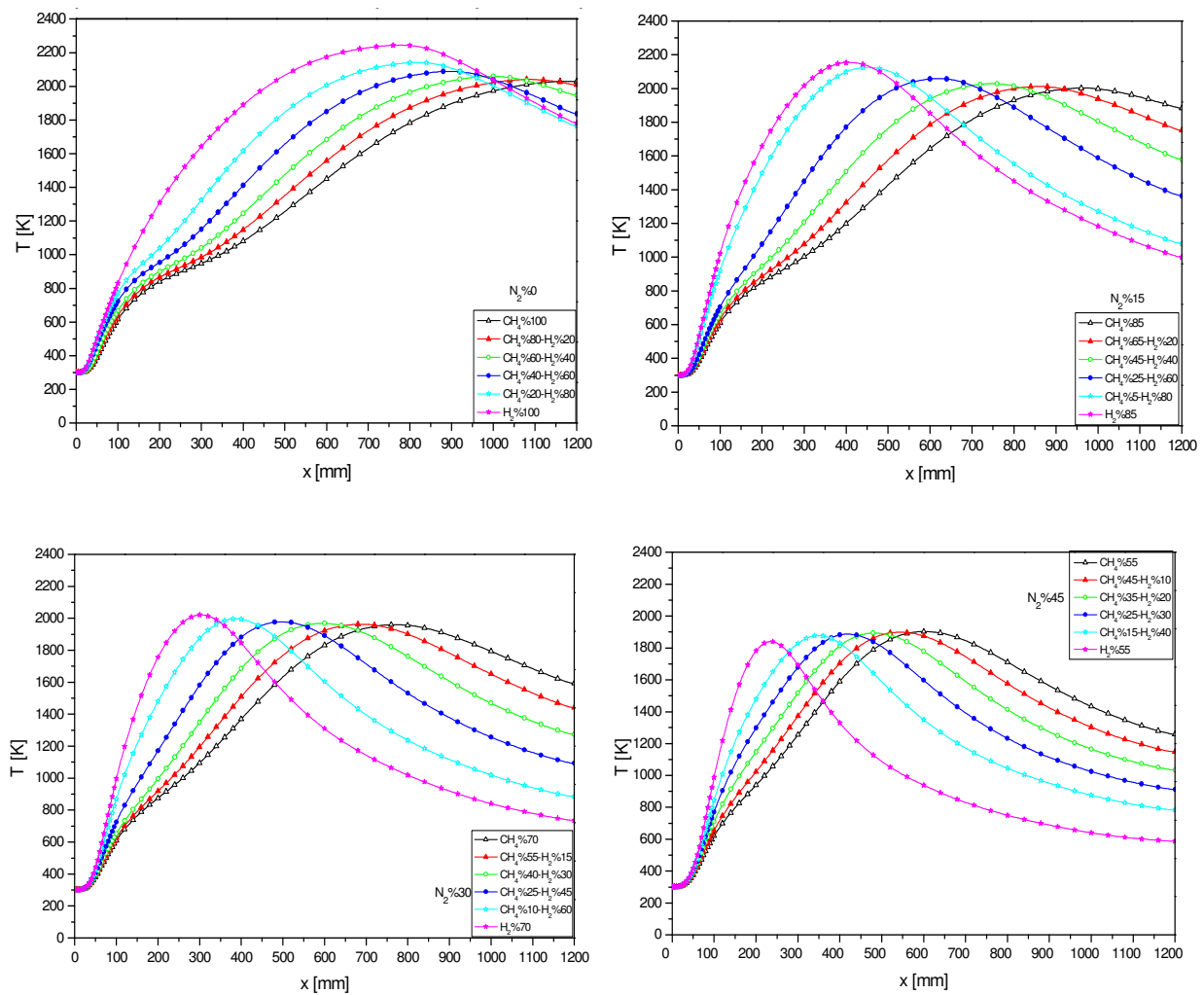
Figure 9. Predicted centerline temperature profiles

Figure 10 shows the flame lengths in relation to %H_2 and %N_2. As shown from this figure, both H_2 and N_2 addition to the mixture decreases the flame length. Flame lengths were obtained from Figure 9, assuming flame length corresponds to the axial position of the peak flame temperature. Also calculations were performed at 15%N_2, 30%N_2, and 45% N2 with adjustments to the volumetric flow of fuel to give the same energy as those provided under 0% N2 conditions. The results showed that increasing the volumetric flow of fuel increased the flame length at a negligible level.
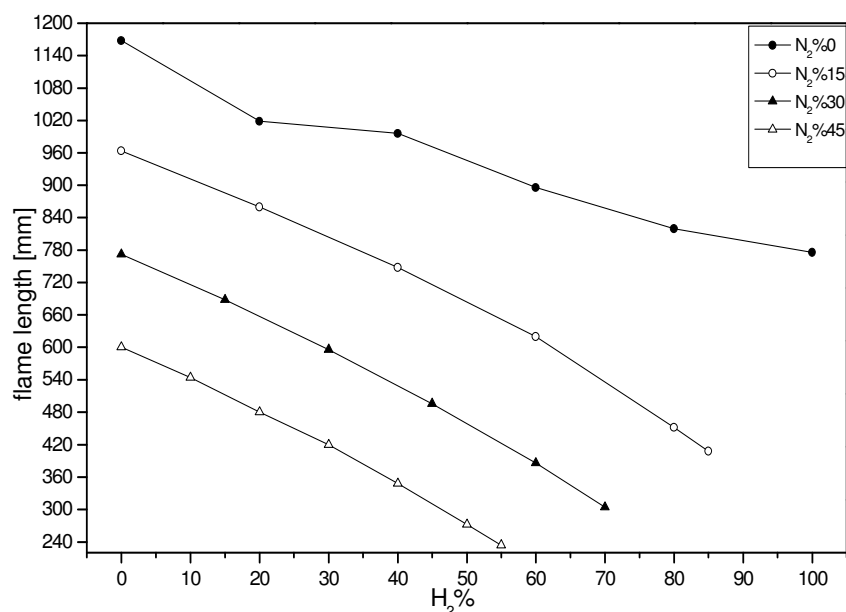
Figure 10. Predicted flame length in relation to $\%H_2$ and $\%N_2$

5. Conclusions

In this study, numerical simulation of a turbulent $H_2/CH_4/N_2$ composite fuel diffusion flame was performed to predict the temperature, axial velocity, and CO_2 concentration distributions. For model validation, the numerical results were compared with the experimental data taken from literature. Also, the effect of varying the hydrogen and nitrogen content of the mixture on combustion was investigated. Grids were created at different numbers. A non-uniform grid with 57,200 meshes was used for calculations. It was found that finer grids had negligible changes on the simulation results. For the validation case, calculations with radiation and without radiation did not affect the solution significantly. Predicted temperature values were generally higher than were the experimental results. In connection with this temperature distribution, numerical CO_2 concentration values were generally higher than the experimental results. Generally, the model results for temperature, velocity, and CO_2 concentration distributions were in satisfactory agreement with the experimental results. Differences between the experimental and numerical results could occur because of the complexity of the real combustion reactions, which cannot be reflected by the reaction mechanism, the equilibrium assumption in the solution procedure, and the turbulence model deficiency that was used in calculations. The numerical results showed that adding hydrogen to the fuel mixture decreases the flame length and generally increases the maximum temperature of the flame. On the other hand, N_2 addition to the mixture decreases both the flame length and maximum flame temperature. It was also observed that increasing the volumetric flow of fuel does not have a significant effect on flame length.

References

Bergmann V., Meier W., Wolff D., Stricker W. (1998) 'Application of spontaneous Raman and Rayleigh scattering and 2D LIF for the characterization of a turbulent $CH_4/H_2/N_2$ jet diffusion flame', *Applied Physics B*, Vol. 66, pp.489–502.

Choudhuri A.R. and Gollahalli S.R. (2003) 'Characteristics of hydrogen–hydrocarbon composite fuel turbulent jet flames', *International Journal of Hydrogen Energy*, Vol. 28, pp.445-454.

El-Ghafour S.A.A., El-Dein A.H.E., Aref A.A.R. (2010) 'Combustion characteristics of natural gas–hydrogen hybrid fuel turbulent diffusion flame', *International Journal of Hydrogen Energy*, Vol. 35, pp.2556-2565.

Fluent Inc. (2006) 'Fluent 6.3 User's Guide', Lebanon NH, USA.

Francis K.A., Sreenivasan R., Raghavan V. (2011) 'Investigation of structures and reaction zones of methane-hydrogen laminar jet diffusion flames', *International Journal of Hydrogen Energy*, Vol. 36, pp.11183-11194.

Frassoldati A., Firgerio S., Colombo E., Inzoli F., Faravelli T. (2005) 'Determination of NO_x emissions from strong swirling confined flames with an integrated CFD–based procedure', *Chemical Engineering Science*, Vol. 60, pp.2851–2869.

Ilbaş M., Yılmaz I., Veziroglu T.N., Kaplan Y. (2005) 'Hydrogen as burner fuel: modelling of hydrogen–hydrocarbon composite fuel combustion and NO_x formation in a small burner', *International Journal of Energy Research*, Vol. 29, pp.973-990.

Khelil A., Naji H., Loukarfi L., Mompean G. (2009) 'Prediction of a high swirled natural gas diffusion flame using a PDF model', *Fuel,* Vol. 88, pp.374–381.

Meier W., Barlow R.S., Chen Y.L., Chen J.Y. (2000) 'Raman/Rayleigh/LIF measurements in a turbulent $CH_4/H_2/N_2$ jet diffusion flame: Experimental techniques and turbulence–chemistry interaction', *Combustion and Flame*, Vol. 123, pp.326–343.

Neuber A., Krieger G., Tacke M., Hassel E., Janicka J. (1998) 'Finite rate chemistry and NO mole fraction in non-premixed turbulent flames', *Combustion and Flame*, Vol. 113, pp.198–211.

Patankar S. (1980) 'Numerical Heat Transfer and Fluid Flow', Hemisphere Publishing Corporation, New York, USA.

Sandia National Laboratories (2013) Available at http://ca.sandia.gov/tdf/Workshop.html (accessed on January 2013).

Tabet F., Sarh B., Gokalp I. (2009) 'Hydrogen–hydrocarbon turbulent non-premixed flame structure', *International Journal of Hydrogen Energy*, Vol. 34, pp.5040-5047.

Zhou X., Sun Z., Brenner G., Durst F. (2000) 'Combustion modeling of turbulent jet diffusion H_2/air flame with detailed chemistry', *International Journal of Heat and Mass Transfer,* Vol. 43, pp.2075-2088.